



# Structure and Morphology of Uric Acid by Orthosiphon Aristatus

Yuni Warty<sup>1\*</sup>, Dewi Wulandari<sup>1</sup>, Eviyona Laurante Br Barus<sup>1</sup>

<sup>1</sup> Faculty of Mathematics and Natural Sciences, Medan State University, Indonesia.

Received: January 17, 2024

Revised: August 19, 2024

Accepted: March 25, 2025

Published: March 31, 2025

Corresponding Author:

Yuni Warty

[yuniwarty@gmail.com](mailto:yuniwarty@gmail.com)

DOI: [10.29303/jppipa.v11i3.6995](https://doi.org/10.29303/jppipa.v11i3.6995)

© 2025 The Authors. This open access article is distributed under a (CC-BY License)



**Abstract:** Urolithiasis is stone-like material that settles in the urinary tract. The materials that make up urinary stones are calcium oxalate, uric acid, cystine and stuvite. Several medical procedures are often applied to cure this disease. However, many patients choose traditional treatment by consuming herbal medicine. The aim of this research is to show the structure and morphology of uric acid with Orthosiphon aristatus. This is very important to study as a basis for producing herbal medicines in nanometer sizes. Samples were prepared before characterization. Urid Acid and Orthosiphon aristatus samples were weighed at a ratio of 0.1: 0.5 milligrams and dissolved in 100 milliliters of Aquabides. The samples were then characterized using XRD and SEM-EDX uric acid crystals mixed with Orthosiphon aristatus undergo progressive dissolution, characterized by an increasingly smooth surface and smaller particle size over time. The particle diameter of each sample changed from 37.64 to 32.83. This research will contribute to urinary stone sufferers choosing appropriate traditional medicine for the type of urinary stone they have.

**Keywords:** Orthosiphon aristatus; Uric acid; Urinary stone

## Introduction

Urolithiasis is known as kidney stone disease in Indonesia. This disease occurs in the urinary tract due to the formation of crystal aggregates. Kidney stones have been identified since ancient Greek times (Modlin, 1980; Warty, Haryanto, Fitri, Maulana, et al., 2020). Indonesia as a developing country has a large number of sufferers, one of the large hospitals in the center of the country reported 5,174 cases of kidney stones in six years with a stone size of around  $11.90 \pm 7.54$  mm (Noviandini et al., 2015). Other developed and developing countries also report varying cases such as 1-5% in Asia, 5-9% in Europe, 13% in North America, 20% in Saudi Arabia (Jing et al., 2010). This disease is also the third most common disease case in urology departments worldwide (Selvaraju et al., 2012; Warty, Haryanto, Fitri, Haekal, et al., 2020).

The condition of lack of fluid in the urinary tract or supersaturation is the main cause of kidney stone formation (Felizio et al., 2022; Fitri et al., 2020; Fukuhara

et al., 2016; Warty et al., 2019). Some patients only realize that they have kidney stones after they are millimeters or centimeters in size. However, when viewed from the formation process, kidney stones are formed from nanometer-sized crystals which then form aggregates if supersaturation or other conditions are found in the urinary tract (He et al., 2010; Khan et al., 2004). Various types of crystals can be found in kidney stones. Some of the most common types are oxalate, phosphate, uric acid, cysteine (Menon et al., 1998). The prevalence of kidney stone disease worldwide ranges from 4%-8% (Curhan et al., 1994; Hesse et al., 1997; Hussein et al., 2013; Sreenevasan, 1981). Therefore, the treatment of this disease is an important concern in the field of urology. Medical therapy for kidney stones is usually carried out with a multidimensional approach that aims to reduce risk factors for patients. Common therapies include limiting sodium intake, reducing animal protein consumption, reducing calcium and oxalate intake, and increasing fluid intake (Felizio et al., 2022; Finger et al., 2023; Lemoine et al., 2023). Chemical drugs are also often

## How to Cite:

Warty, Y., Wulandari, D., & Barus, E. L. B. (2025). Structure and Morphology of Uric Acid by Orthosiphon Aristatus. *Jurnal Penelitian Pendidikan IPA*, 11(3), 1147-1152. <https://doi.org/10.29303/jppipa.v11i3.6995>

used for this medical therapy such as potassium citrate, antibiotics, and others. In addition to medical treatment, patients also choose to take herbal medicines such as Orthosiphon Aristatus (Chitme, 2010; Putri et al., 2024). Orthosiphon Aristatus contains terpenoids, polyphenols, and sterols with three compounds, namely sinensetin, eupatorin, 3'-hydroxy-5,6-74 tetramethoxiflavone, and rosmarinic acid. With the content of compounds owned by Orthosiphon Aristatus, this plant can inhibit the formation of kidney stones and prevent the growth of kidney stones.

The therapeutic potential of gout by Orthosiphon aristatus can be seen from its structure. Research shows that compounds from Orthosiphon aristatus, such as sinensetin, can inhibit gout through interactions with certain proteins, thereby increasing its role in gout therapy. Molecular studies revealed binding affinities indicating effective inhibition of uric acid reabsorption (Faridah et al., 2023). Orthosiphon aristatus shows antiulcerolytic effects, which can indirectly affect uric acid levels by preventing the formation of kidney stones. In vitro studies showed 78.06% efficacy in inhibiting the formation of calcium oxalate crystals, indicating a dual role in managing urinary tract health (Porchezhiyan et al., 2023). The molecular structure of uric acid can form clusters with water, which affects its solubility and interaction with biological systems (Cai et al., 2023). In addition, the diuretic properties of Orthosiphon aristatus are known to help excrete uric acid, thereby preventing the formation of uric acid stones by increasing urine alkalinity (Nirdnoy et al., 1991).

The morphology of Orthosiphon aristatus contributes to increasing diuresis which helps eliminate excess uric acid from the body (Sianipar et al., 2020). Uric acid levels can be reduced by this plant because it can inhibit xanthine oxidase (XO), an enzyme involved in the production of uric acid (Nurihardiyanti et al., 2022).

Understanding the morphology of uric acid crystals by Orthosiphon aristatus may reveal how the plant affects the solubility and excretion of uric acid, which contributes to its therapeutic efficacy. Detailed knowledge of the structural interactions between uric acid and compounds in Orthosiphon aristatus may guide the development of more effective treatments for hyperuricemia and related disorders. Investigating how Orthosiphon aristatus alters uric acid crystallization may open up opportunities to combine it with other treatments to enhance its efficacy. Understanding how Orthosiphon aristatus affects uric acid crystal morphology may help in developing strategies to prevent its formation or accelerate its dissolution. Studying the changes in uric acid morphology in the presence of plant extracts may provide insight into how natural compounds modify crystal growth, aggregation, and stability. Therefore, experimental studies are

needed to investigate the effects of Orthosiphon aristatus on uric acid crystals in vitro.

## Method

### Materials

The tools and materials used in this study are Nano Particle Analyzer Horiba SZ-100 which is used to measure particle size in solution. Scanning electron microscope to see the morphology of the sample that has been prepared in powder form. X-ray diffraction to characterize the structure of the material. Ultrasound to stir the solution during preparation, cuvette, Iwaki Pyrex 250 ml measuring cup, Iwaki CTE 250 ml beaker, 5 ml Syringe, AND GR-200 digital scale, 3 Micrometer microporous membrane and 1.2 micrometer filter paper. While the materials needed in this experiment are uric acid crystals, Orthosiphon Aristatus MTA-36085657 extract and Aquabides.

### Sample Preparation and Data Acquisition

Urid Acid was cleaned from biological cell residues using 95% alcohol and dried at 40 °C for 30 minutes. A mortar was used to grind the sample into powder form (Permatasari, 2021). Urid Acid and Orthosiphon aristatus samples were weighed at a ratio of 0.1: 0.5 milligrams and dissolved in 100 milliliters of Aquabides. The samples were made in five parts, namely at time intervals of 0, 60, 120, 180, 240 minutes. Each was stirred using ultrasound for solution homogeneity, some of the solution was put into a cuvette to measure particles using a 3 µm microporous membrane. Each sample was ultrasounded at a predetermined time interval the other solution was filtered using 1.2 µm filter paper and dried in an oven at 40°C for 15 minutes. The samples were then characterized using XRD and SEM-EDX. Analysis of crystal structure, crystal size and elemental composition is the final goal.

## Result and Discussion

### Sample Preparation Results

Sample preparation begins by washing the sample with aquabides which aims to remove biological contaminants such as proteins, lipids, or dead cells that can interfere with analysis or chemical reactions. Avoiding Analytical Interference by ensuring that the results obtained only come from the compounds or samples to be analyzed. Increasing Sample Stability so that there is no sample degradation or triggering the growth of microorganisms observation time or characterization of the sample after being left for 0 minutes to 240 minutes. This treatment aims to study Reaction Kinetics by determining the reaction rate between uric acid and active compounds in Orthosiphon

aristatus from changes in particle size. In addition to ensuring whether Orthosiphon aristatus is able to dissolve or reduce the size of uric acid crystals within a certain time. This is important in the development of medical or pharmaceutical applications, such as herbal medicines for gout disorders.

### Morphology

The morphology of each sample can be seen as in Figure 1. From this figure, it can be seen that there are changes in morphology at each time placement. From time  $t=0$  to  $t=4$ , the structure is more evenly distributed.

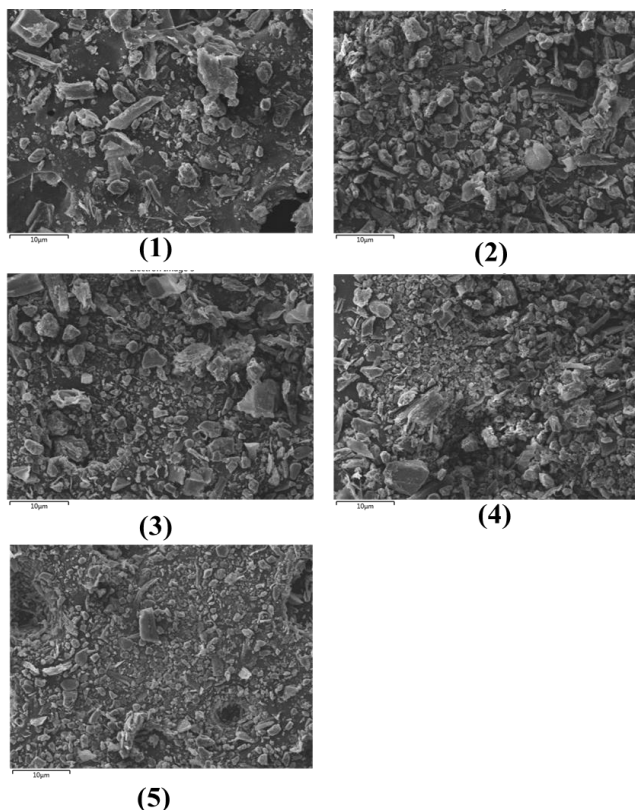


**Figure 1.** Sample Morphology (1) sample  $t=0$  hours, (2) sample  $t=1$  hour, (3) sample  $t=2$  hours, (4) sample  $t=3$  hours (5) sample  $t=4$  hours

Figure 1 shows at  $t = 0$  hours the crystal surface looks rough with sharp edges and clear corners, this reflects the original crystal structure. While the particle size tends to be large, with uniform dimensions and no signs of dissolution or degradation. The shape of uric acid crystals changes with the drying rate and the morphology of nanoparticles is greatly influenced by the drying kinetics. Nanonuclei are amorphous but can grow into micron-sized crystalline particles. The morphology of uric acid nanonuclei is significantly different from that of supermicron-sized crystalline particles. This implies that the solubility characteristics, surface properties, elimination, and medical treatment

of uric acid nanonuclei formed during the early stage of nucleation should be reconsidered (Rastogi et al., 2022). In sample 2 with  $t = 1$  (60 minutes) the surface begins to show signs of erosion, with small smoother areas appearing in some parts and the particle size decreases slightly, indicating the beginning of the dissolution process marked by some particles starting to break into smaller fragments. In sample 3,  $t = 2$  (120 minutes) Surface erosion is getting smoother and there is an uneven dissolution pattern across the surface and the particles become smaller and more fragments are visible, reflecting the cumulative effect of the dissolution process. In sample 4,  $t = 3$  (180 minutes) The surface is getting smoother and a thin layer is visible which appears to come from the active compound Orthosiphon aristatus that coats or reacts with the crystals. The particle size is also getting smaller, with the dominance of fine fragments among the remaining particles at pointment 5,  $t=4$  (240 Minutes). The surface is almost completely smooth, indicating a dissolution process approaching saturation. The remaining particle structure appears much smaller and less defined. The particles become very small, with a more even size distribution compared to the previous time.

SEM observations show that uric acid crystals mixed with Orthosiphon aristatus undergo progressive dissolution, characterized by an increasingly smooth surface and smaller particle size over time. SEM can detect and analyze a wide variety of materials ranging from amorphous substances to microcrystals to macroscopic stones well (Khan et al., 2004). This reflects the effectiveness of the active compounds in Orthosiphon aristatus to dissolve or erode uric acid crystals.

### The Cristal Structure

The results of XRD analysis show that uric acid by Orthosiphon Aristatus in Figure 2 has four domain fields represented by consecutive fields identified according to the JCPDS standard card in samples 1 to five with stirring time from  $t=0$  to  $t=4$  have the same crystal fields namely; (011), (211), (102), and (231). Changes in intensity seen in each sample indicate differences in crystal group, lattice shape, symmetry, unit cell parameters, and the distribution and shape of atoms in the unit cell.

The crystal size of each sample can be seen in table 1. The table shows a change in particle size for each sample. This indicates the reaction or effect of Orthosiphon Aristatus on uric acid crystals. The longer the solution reacts, the smaller the particle size. This is in accordance with the results of previous studies which showed a change in particle size each time using a particle size analyzer.

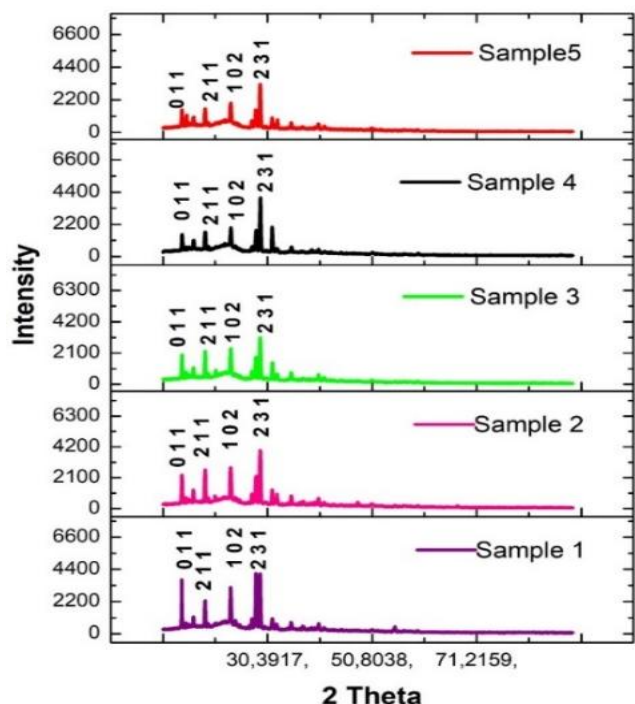


Figure 2. XRD spectrum of uric acid by Orthosiphon Aristatus

Table 1. FWHM and Particle Size of Uric Acid by Orthosiphon Aristatus

Sample	Peak 2θ (degree)	FWHM (rad)	Size (nm)
Sample 1	28.93	0.22	37.64
Sample 2	28.97	0.22	36.80
Sample 3	28.94	0.23	36.47
Sample 4	28.99	0.23	36.31
Sample 5	28.93	0.25	32.83

## Conclusion

Uric acid crystals mixed with Orthosiphon aristatus undergo progressive dissolution, characterized by an increasingly smooth surface and smaller particle size over time.

## Acknowledgments

The author expresses his gratitude to Medan State University DIPA Funding. In accordance with the Decree of the Chancellor of UNIMED No. 0026/UN33.8/PPKM/PT.

## Author Contributions

Conceptualization, formal analysis and investigation, Y. W; methodology, data curation, and validation, D. W; resources, original draft preparation, writing—review and editing, E. L. B.

## Funding

This research was funded by Lembaga Penelitian dan Pengabdian kepada Masyarakat (LPPM) Universitas Negeri Medan.

## Conflicts of Interest

The authors declare no conflict of interest related to the publication of this article.

## References

Cai, Z., Zhu, C., Chen, G., Wu, Y., Gu, J., Ma, C., Gao, H., Li, L., & Guo, S. (2023). Study on intermolecular hydrogen bond of uric acid water-clusters. *Chemical Physics Letters*, 818, 140424. <https://doi.org/10.1016/j.cplett.2023.140424>

Chitme, H. R. (2010). Herbal treatment for urinary stones. *International Journal of Pharmaceutical Sciences and Research*, 1(2), 24–31. Retrieved from [https://kevaind.org/download/Dolichos Biflorus on kidney.pdf](https://kevaind.org/download/Dolichos_Biflorus%20on%20kidney.pdf)

Curhan, G. C., Rimm, E. B., Willett, W. C., & Stampfer, M. J. (1994). Regional variation in nephrolithiasis incidence and prevalence among United States men. *Journal of Urology*, 151(4), 838–841. [https://doi.org/10.1016/S0022-5347\(17\)35101-7](https://doi.org/10.1016/S0022-5347(17)35101-7)

Faridah, A., Verawati, R., Oktavia, B., Ghufron, M., Purnamasari, D., Ghifari, M. R., Rosalina, L., Azhari, P., Zainul, R., Kharisma, V. D., Jakhmola, V., Rebezov, M., & Ansori, A. (2023). Study on the Inhibition of Sinensetin Extract from Cat's Whiskers Plant (Orthosiphon aristatus) on ATP Binding Cassette Sub-Family G Member 2 in Uric Acid. *Pharmacognosy Journal*, 15(4), 506–511. <https://doi.org/10.5530/pj.2023.15.110>

Felizio, J., & Atmoko, W. (2022). Medical Management of Kidney Stones: a review. *Bali Medical Journal*, 11(1), 127–136. <https://doi.org/10.15562/bmj.v11i1.3343>

Finger, M., Finger, E., Bellucci, A., & Malieckal, D. A. (2023). Medical management for the prevention of kidney stones. *Postgraduate Medical Journal*, 99(1169), 112–118. <https://doi.org/10.1136/postgradmedj-2021-140971>

Fitri, L. A., Haryanto, F., Arimura, H., YunHao, C., Ninomiya, K., Nakano, R., Haekal, M., Warty, Y., & Fauzi, U. (2020). Automated classification of urinary stones based on microcomputed tomography images using convolutional neural network. *Physica Medica*, 78, 201–208. <https://doi.org/10.1016/j.ejmp.2020.09.007>

Fukuhara, H., Ichianagi, O., Kakizaki, H., Naito, S., & Tsuchiya, N. (2016). Clinical relevance of seasonal changes in the prevalence of ureterolithiasis in the diagnosis of renal colic. *Urolithiasis*, 44(6), 529–537. <https://doi.org/10.1007/s00240-016-0896-3>

He, J.-Y., Deng, S.-P., & Ouyang, J.-M. (2010). Morphology, Particle Size Distribution, Aggregation, and Crystal Phase of Nanocrystallites

in the Urine of Healthy Persons and Lithogenic Patients. *IEEE Transactions on NanoBioscience*, 9(2), 156–163.  
<https://doi.org/10.1109/TNB.2010.2045510>

Hesse, A., & Siener, R. (1997). Current aspects of epidemiology and nutrition in urinary stone disease. *World Journal of Urology*, 15(3), 165–171.  
<https://doi.org/10.1007/BF02201853>

Hussein, N. S., Sadiq, S. M., Kamaliah, M. D., Norakmal, A. W., & Gohar, M. N. (2013). Twenty-four-hour urine constituents in stone formers: a study from the northeast part of Peninsular Malaysia. *Saudi Journal of Kidney Diseases and Transplantation: An Official Publication of the Saudi Center for Organ Transplantation, Saudi Arabia*, 24(3), 630–637.  
<https://doi.org/10.4103/1319-2442.111090>

Jing, Z., GuoZeng, W., Ning, J., JiaWei, Y., Yan, G., & Fang, Y. (2010). Analysis of urinary calculi composition by infrared spectroscopy: a prospective study of 625 patients in eastern China. *Urological Research*, 38(2), 111–115.  
<https://doi.org/10.1007/s00240-010-0253-x>

Khan, S. R., & Kok, D. J. (2004). Modulators of urinary stone formation. *Frontiers in Bioscience*, 9, 1450–1482. <https://doi.org/10.2741/1347>

Lemoine, S., Dahan, P., Haymann, J. P., Meria, P., & Almeras, C. (2023). 2022 Recommendations of the AFU Lithiasis Committee: Medical management – from diagnosis to treatment. *Progrès En Urologie*, 33(14), 911–953.  
<https://doi.org/10.1016/j.purol.2023.08.004>

Menon, M., Parulkar, B. G., & Drach, G. W. (1998). Urinary Lithiasis: Etiology, Diagnosis and Medical Management. In *Campbell's Urology* (Vol. 3, p. 2702). W. B. Saunders Co.

Modlin, M. (1980). A history of urinary stone. *South African Medical Journal*, 58(16), 652–655. Retrieved from <https://shorturl.at/Z70XC>

Nirdnoy, M., & Muangman, V. (1991). Effects of Folia orthosiphonis on urinary stone promoters and inhibitors. *Journal of the Medical Association of Thailand: Chotmaihet Thangphaet*, 74(6), 318–321. Retrieved from <http://www.ncbi.nlm.nih.gov/pubmed/1744535>

Noviandrinini, E., Birowo, P., & Rasyid, N. (2015). Urinary stone characteristics of patients treated with extracorporeal shock wave lithotripsy in Cipto Mangunkusumo Hospital Jakarta, 2008–2014: a gender analysis. *Medical Journal of Indonesia*, 24(4), 234–238. <https://doi.org/10.13181/mji.v24i4.1258>

Nurihardiyanti, N., Sari, A. K., & Amalia, T. R. (2022). Aktivitas Antihiperurisemia Kombinasi Ekstrak Daun Kumis Kucing (Orthosipon aristatus var. Aristatus L.) dan Daun Tempuyung (Sonchus arvensis L.) secara In Vitro. *Camellia: Clinical, Pharmaceutical, Analytical and Pharmacy Community Journal*, 1(2), 31–37. <https://doi.org/10.30651/cam.v1i2.16740>

Permatasari, A. A. (2021). Diagnostik Urolithiasis. *MEDFARM: Jurnal Farmasi Dan Kesehatan*, 10(1), 35–46.  
<https://doi.org/10.48191/medfarm.v10i1.53>

Porchezhiyan, V., Deen, K., Barani, M., Wilson, S., Pandikumar, P., Ignacimuthu, S., Alharbi, N., & Thiruvengadam, M. (2023). Comparing in vitro antiurolithic potential of Orthosiphon aristatus (Blume) Miq. var. aristatus and its local substitute, Ocimum filamentosum Forssk. *Journal of Research in Siddha Medicine*, 6(2), 78.  
[https://doi.org/10.4103/jrsm.jrsm\\_26\\_23](https://doi.org/10.4103/jrsm.jrsm_26_23)

Putri, I. T. H., Rustini, Ismed, F., Sardi, V. F., & Arifah, N. (2024). Isolation and Inhibitory Activity Testing of Alpha-Glucosidase Enzyme from Endophytic Bacteria in Kumis Kucing (Orthosiphon aristatus (Blume) Miq.) Leaves. *Jurnal Penelitian Pendidikan IPA*, 10(10), 7873–7884.  
<https://doi.org/10.29303/jppipa.v10i10.9264>

Rastogi, D., & Asa-Awuku, A. (2022). Size, Shape, and Phase of Nanoscale Uric Acid Particles. *ACS Omega*, 7(28), 24202–24207.  
<https://doi.org/10.1021/acsomega.2c01213>

Selvaraju, R., Thiruppathi, G., & Raja, A. (2012). FT-IR spectral studies on certain human urinary stones in the patients of rural area. *Spectrochimica Acta - Part A: Molecular and Biomolecular Spectroscopy*, 93, 260–265. <https://doi.org/10.1016/j.saa.2012.03.028>

Sianipar, N. F., & Mariska, I. (2020). Micropropagation Of Orthosiphon Aristatus Through Indirect And Direct Organogenesis. *Jurnal Teknologi*, 82(3).  
<https://doi.org/10.11113/jt.v82.13887>

Sreenevasan, G. (1981). Incidence of urinary stones in the various states of mainland Malaysia. *Medical Journal of Malaysia*, 36(3), 142–147. Retrieved from <https://pubmed.ncbi.nlm.nih.gov/7329370/>

Warty, Y., Fitri, L. A., Haryanto, F., & Herman. (2019). Development of light scattering methods for urinary stones diagnosis. *Journal of Physics: Conference Series*, 1248(1), 012015.  
<https://doi.org/10.1088/1742-6596/1248/1/012015>

Warty, Y., Haryanto, F., Fitri, L. A., Haekal, M., & Herman, H. (2020). A spatial distribution analysis on the deposition mechanism complexity of the organic material of kidney stone. *Journal of Biomedical Physics and Engineering*, 10(3), 273–282.  
<https://doi.org/10.31661/jbpe.v0i0.1104>

Warty, Y., Haryanto, F., Fitri, L. A., Maulana, R., & Herman. (2020). Urinary Stones Clustering on each layer based on Hounsfield Units Values from Micro CT-SkyScan Images. *Journal of Physics*: 1151

*Conference Series*, 1428(1), 12001.  
<https://doi.org/10.1088/1742-6596/1428/1/012001>